Fish and Shellfish Immunology 84 (2019) 998–1006

Contents lists available at ScienceDirect

Fish and Shellfish Immunology

journal homepage: www.elsevier.com/locate/fsi

Full length article

cDNA cloning, characterization, and expression analysis of the *Rac1* and *Rac2* genes from *Cynoglossus semilaevis*

Yunji Xiu[a,b,c], Hongxiang Zhang[a,b,c,d], Shuangyan Wang[b,c,d], Tian Gan[b,c,d], Min Wei[b,c], Shun Zhou[a], Songlin Chen[b,c,*]

[a] Marine Science and Engineering College, Qingdao Agricultural University, Qingdao, 266109, China
[b] Laboratory for Marine Fisheries Science and Food Production Processes, Qingdao National Laboratory for Marine Science and Technology Yellow Sea Fisheries Research Institute, CAFS, Qingdao, 266071, China
[c] Key Lab of Sustainable Development of Marine Fisheries, Ministry of Agriculture, Qingdao, 266071, China
[d] College of Fisheries and Life Science, Shanghai Ocean University, Shanghai, 201306, China

ARTICLE INFO

Keywords:
Small Rho GTPase
Rac1
Rac2
Cynoglossus semilaevis
Innate immunity

ABSTRACT

Rac1 and Rac2, belonging to the small Rho GTPase family, play an important role during the immune responses. In this study, a *Rac1* homolog (*CsRac1*) and a *Rac2* homolog (*CsRac2*) were cloned from the *Cynoglossus semilaevis*. The full-length of *CsRac1* and *CsRac2* cDNA was 1219 bp and 1047 bp, respectively. Both *CsRac1* and *CsRac2* contain a 579 bp open reading frame (ORF) which encoding a 192 amino acids putative protein. The predicted molecular weight of *CsRac1* and *CsRac2* was 21.41 kDa and 21.35 kDa, and their theoretical pI was 8.50 and 7.91, respectively. Sequence analysis showed that the conserved RHO domain was detected both from amino acid of *CsRac1* and *CsRac2*. Homologous analysis showed that *CsRac1* and *CsRac2* share high conservation with other counterparts from different species. The *CsRac1* and *CsRac2* transcript showed wide tissue distribution, in which *CsRac1* and *CsRac2* exhibit the highest expression level in liver and gill, respectively. The expression level of *CsRac1* and *CsRac2* fluctuated in the liver and gill tissues at different time points after challenged by *Vibrio harveyi*. Specifically, *CsRac1* and *CsRac2* were significantly up-regulated at 48 h and 96 h post injection. Moreover, the knocking down of *CsRac1* and *CsRac2* in cell line (TSHKC) reduced the expression of *CsPAK1, CsIL1-β* and *CsTNF-α*. The present data suggests that *CsRac1* and *CsRac2* might play important roles in the innate immunity of half-smooth tongue sole.

1. Introduction

The mammalian Rho GTPases consist of twenty-two homologous proteins, which can be divided into eight subgroups: *Rho* (*RhoA*, *RhoB*, *RhoC*), *Rac* (*Rac1*, *Rac2*, *Rac3*, *RhoG*), *Cdc42* (*Cdc42*, *TC10*, *TCL*, *Chp*, *Wrch-1*), *Rnd* (*Rnd1*, *Rnd2*, *Rnd3/RhoE*), *RhoD* (*RhoD*, *Rif*), *RhoH/TTF*, *RhoBTB* (*RhoBTB1*, *RhoBTB 2*) and *Miro* (*Miro-1*, *Miro-2*) [1]. Similar to other reported GTPases, Rho GTPases act as molecular switches cycling between the inactive GDP-bound state and active GTP-bound state [2,3]. Their activity was affected by GTPase-activating proteins, guanine-nucleotide-exchange factors and guanosinenucleotide-dissociation inhibitors [4]. Rho small GTPases participated in many important cellular processes, such as cytoskeletal organization, transcription, cell proliferation, differentiation, phagocytosis and NADPH oxidase activation [5–10]. In addition, they play important roles in the infection process of different pathogens [11].

As a subfamily of Rho GTPases, Rac (ras-related C3 botulinum toxin substrate) consists of four members, including *Rac1*, *Rac2*, *Rac3* and *RhoG*. Among them, the Rac1 is ubiquitously expressed and shares 92% amino acid identity with hematopoietic-specific Rac2 [12]. It has been widely reported that *Rac1* and *Rac2* participated in the host's immune response against bacterial infection. Rac1 and Rac2 play important rols both in humoral and cellular immune responses, in which, they could regulate B cell homotypic adhesion and Ig class switching [13], T-cell development [14], phagocytic ability of phagocytic cells [15] and so on.

The function of Rac GTPases has been fully studied in mammals, but few researches have been done in teleost. *Rac1* has only been cloned and functionally characterized in *Ctenopharyngodon idella* [16], *Scophthalmus maximus* [17], *Danio rerio* [18] and *Pseudosciaena crocea* [19]; *Rac2* has only been cloned and functionally characterized in *Larimichthys crocea* [20]. Except in zebrafish, all of the *Rac1* transcripts

* Corresponding author. Yellow Sea Fisheries Research Institute, Chinese Academy of Fishery Sciences (CAFS), Qingdao, 266071, China.
E-mail address: chensl@ysfri.ac.cn (S. Chen).

https://doi.org/10.1016/j.fsi.2018.11.006
Received 9 May 2018; Received in revised form 26 October 2018; Accepted 1 November 2018
Available online 03 November 2018
1050-4648/

Table 1
Primers used in this research.

Primer	Sequence (5′ – 3′)
CsRac1-5′RACE-R1	GCGTTGGTGGTGTAGCTGATAAGAAGACA
CsRac2-5′RACE-R1	GGCTCACCAGGGAGAAGCAGATTAGGA
CsRac1-3′RACE-F1	AGCTGGACCTGAGGGACGACAAGG
CsRac2-3′RACE-F1	CGTCCTACGAGAACGTCAGAGCAAAGTG
CsRac1-RT-F1	GCCGAGACAAACAGAGGGAAAG
CsRac1-RT-R1	TCAACCATCACATTGGCAGAGTAG
CsRac2-RT-F1	GAGGGCAAAGAGCGCAGA
CsRac2-RT-R1	CAGAGTAGTTGTCAAATACAGTAGGAATGTA
Beta-actin-F	GCTGTGCTGTCCCTGTA
Beta-actin-R	GAGTAGCCACGCTCTGTC
siRNA-CsRac1	AGTCCAGCTTCCTTCGAAA
siRNA-CsRac2	ACAACTACTCTGCTAACGT
CsPAK1-F1	CTGGAGATGGATGTGGAGAAGAG
CsPAK1-R1	AGGAGTGAGACTGGAGAGAGGCT
CsIL-1b-F1	GAAGTGACGACCTGAGATTTTTGT
CsIL-1b-R1	TCCTTGGCTGTGCTGATGAAC
CsIFNa3-F1	GTCTTGTTGGTTTGCCTCTTCCT
CsIFNa3-R1	GCAGAATCTTTATCTGCCTGACTGTAG

showed wide tissue distribution and were fluctuated by bacteria or PAMPs stimulations. It was elucidated that *Rac1* could activate NF-kB signaling [16]. qRT-PCR revealed that *Rac2* of *L. crocea* expressed in all detected tissues and its expression in liver, spleen and head-kidney was up regulated obviously after stimulated by LPS, polyI: C or *Vibro parahaemolyticus* [20]. Above all, it has been speculated that both *Rac1* and *Rac2* would participate in the immune responses and play a crucial role in defence against bacteria and virus. However, it still has no research on *Rac1* and *Rac2* of *Cynoglossus semilaevis*.

The half-smooth tongue sole (*C. semilaevis*) is a kind of sea fish with high economic value in the aquaculture industry in northern China. However, with the increasing scale and intensification of aquaculture, the diseases are becoming more and more serious. In this study, the cDNA sequences of *C. semilaevis Rac1* and *Rac2* (named *CsRac1* and *CsRac2*) were identified and characterized. Their amino acid sequences were compared with other known counterparts. The relative expression of *CsRac1* and *CsRac2* in a variety of tissues were analyzed. Furthermore, the time-dependant expression pattern of *CsRac1* and *CsRac2* after challenged with *V. harveyi* were examined both in liver and gill tissues.

2. Materials and methods

2.1. Animal and RNA extraction

The healthy *C. semilaevis* used in this research were collected from Huanghai Aquaculture Company (Haiyang, Shandong, People's Republic of China). The experimental fish were approximately 1.5 years old with an average length of 30.3 cm and an average weight of 250 g. The fish were acclimatized for 7 days before the experiments. The TRIzol reagent (Life Technologies) was used to extract the total RNA of different tissues. RNA quality was measured by agarose gel electrophoresis. The concentration of RNA was assessed by spectrophotometer at 260 nm absorbance.

2.2. Cloning full-length of CsRac1 and CsRac2

The complete cDNA sequences were obtained with the Rapid amplification of the cDNA ends (RACE) method. Gene specific primers were designed based on the corresponding EST sequences. Primer Premier 5.0 software was used to design gene specific primers. For 5′-RACE, amplification was performed with *CsRac1*-5′-RACE-R1 or *CsRac2*-5′-RACE-R1 and Universal Primer A Mix (UPM) (Table 1). For 3′-RACE, the PCR reactions were conducted with *CsRac1*-3′RACE-F1 or *CsRac2*-3′RACE-F1 and UPM (Table 1). The PCR products were cloned into pEASY-T1 vector (Trans, China) and sequenced by Ruibo Biotechnology Company.

2.3. Bioinformatic analysis

In order to identify the nucleotide and amino acid sequence similarities, cDNA sequences of *CsRac1* and *CsRac2* were blasted against NCBI database (http://blast.ncbi.nlm.nih.gov/Blast.cgi). The ORF Finder (http://www.ncbi.nlm.nih.gov/orffinder/) was used to identify the ORF and the SMART (http://smart.embl-heidelberg.de/) was used to predict their functional domains. The Chou & Fasman Secondary Structure Prediction Server (http://www.biogem.org/tool/chou-fasman/) was applied to predict their secondary structures. Three dimensional (3D) structures were predicted by the Swiss-Model Workspace (https://swissmodel.expasy.org/) and then evaluated by Swiss-PdbViewer. Multiple sequences alignment was performed using the DNAMAN program. A neighbor-joining phylogenetic tree was constructed based on the amino sequences alignment by MEGA 5 program.

2.4. Tissue distribution of CsRac1 and CsRac2

The mRNA expression level of *CsRac1* and *CsRac2* in different tissues were determined by qRT-PCR, in which six tissues (liver, spleen, kidney, brain, gill and intestine) were extracted from 3 untreated fish. The first-strand cDNA was synthesized using PrimeScript™ 1st Strand cDNA Synthesis Kit (Takara). Two pairs of primers (*CsRac1*-RT-F1, *CsRac1*-RT-R1 and *CsRac2*-RT-F, *CsRac2*-RT-R) (Table 1) were designed to quantify *CsRac1* and *CsRac2*, respectively. *Beta-actin* expression levels were used as internal control. SYBR® Premix Ex Taq TM II (Tli RNaseH Plus) (Takara) was used to conduct the qRT-PCR experiment. The relative copy number of *CsRac1* and *CsRac2* were calculated following the $2^{-\triangle\triangle Ct}$ method. Statistical analysis was performed using SPSS software (Ver11.0). All data were given as Mean ± S.E. Statistical significance was set at $P < 0.05$, which was determined by one-way ANOVA.

2.5. Expression profiles after V. harveyi challenge

In this experiment, the bacteria *V. harveyi* were isolated from diseased fish and kept in our laboratory. In brief, the bacteria were incubated to mid-logarithmic stage at 28 °C in tryptic soy broth (TSB) medium, then collected by centrifugation and re-suspended in PBS. To determine the expression profiles of *CsRac1* and *CsRac2* following an immune challenge, fish were injected individually with 50 μl live *V. harveyi* suspension (1.0×10^4 cells/ml). Liver and gill tissue samples from 3 fish were isolated at 0, 12, 24, 48, 72 and 96 h post-injection.

2.6. Expression profiles of immune related genes after RNA interference of CsRac1 and CsRac2

The siRNAs specific for *CsRac1* and *CsRac2* were synthesized by Ribobio Corporation (Guangzhou, China), and the sequences are shown in Table 1. Cell line (TSHKC) from head kidney of half-smooth tongue sole in a 24-well plate (1×10^5/well) were transfected with 100 nmol

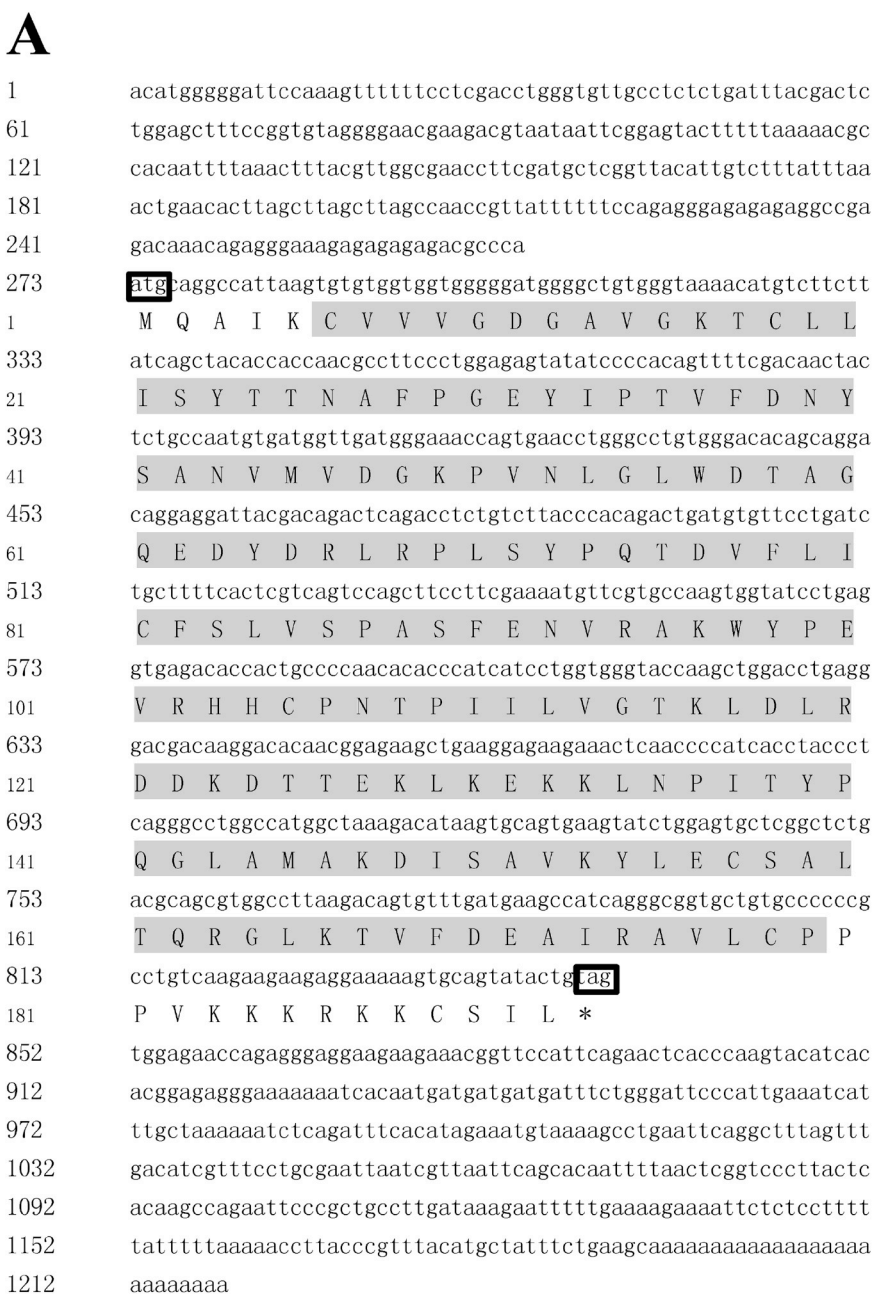

Fig. 1. Nucleotide and deduced amino acid sequence of *CsRac1* (A) and *CsRac2* (B). The numbers on the left represent the nucleotide and deduced amino acid sequences. The letters in boxes indicate the start codon (atg), the stop codon (tag or taa) and the polyadenylation signal sequences (aataaa). The conserved RHO domain is shaded.

of siRNA and 3 μl riboFECT™ CP transfection reagent. The control group was transfected with negative control siRNA. After 30 h, the cells were treated with TRIzol Reagent (Life Technologies). Then, the total RNA was extracted and the first-strand cDNA was synthesized. The RNAi efficiency and expression profiles of immune related genes (*CsPAK1, CsIL1-β* and *CsTNF-α*) were detected by qRT-PCR. Gene specific primers were designed by Primer Premier 5.0 software (Table 1).

3. Results

3.1. Cloning and characterization of CsRac1 and CsRac2

The full-length of *CsRac1* cDNA (GenBank accession No. MH085219) was 1219 bp, containing a 272 bp 5′-untranslated region (UTR) and a 368 bp 3′-UTR with a poly(A) tail. The ORF of *CsRac1* was 579 bp, encoding a protein of 192 amino acids with a calculated molecular weight of 21.41 kDa and a theoretical pI of 8.50. There is 21 negatively (Asp + Glu) charged residues and 26 positively (Arg + Lys) charged residues. Sequence analysis indicated that the *CsRac1* protein contains a conserved RHO domain (residues 6–179), which is the signature of Rho GTPase subfamily member (Fig. 1A). *CsRac1* protein was a nontransmembrane protein without signal peptide (Fig. S1 A and S2 A). Secondary structure predicted that *CsRac1* was a mixed protein which contained 67.7% alpha helix, 42.2% beta pleated sheet and 13.0% beta turn (Fig. S3 A). 3D molecular modeling of CsRac1 was generated based on template of 2rmk.1.A (Fig. S4 A). *CsRac1* showed 94.79% consistency with its template. 192 atoms were involved in the calculation and the root mean square deviation of two superposed

B

```
1       acatgggagggcaaagagcgcagacgaagctgagcggaacagg
44      atgcaggctatcaaatgtgtggtcgtgggagatggagctgtgggtaaaacatgtctcctc
1        M  Q  A  I  K  C  V  V  V  G  D  G  A  V  G  K  T  C  L  L
104     atcagctacaccaccaatgccttccccggggaatacattcctactgtatttgacaactac
21       I  S  Y  T  T  N  A  F  P  G  E  Y  I  P  T  V  F  D  N  Y
164     tctgctaacgtgatggtggacagcaagccggtcaatctgggcctctgggatacagctggg
41       S  A  N  V  M  V  D  S  K  P  V  N  L  G  L  W  D  T  A  G
224     caggaggactacgacaggctgcgtccactgtcctacccacagacggatgttttcctaatc
61       Q  E  D  Y  D  R  L  R  P  L  S  Y  P  Q  T  D  V  F  L  I
284     tgcttctccctggtgagcccagcgtcctacgagaacgtcagagcaaagtggtaccccgag
81       C  F  S  L  V  S  P  A  S  Y  E  N  V  R  A  K  W  Y  P  E
344     gttcgtcatcactgcccctccacgcccatcatcctggtgggcaccaagctggatctgagg
101      V  R  H  H  C  P  S  T  P  I  I  L  V  G  T  K  L  D  L  R
404     gatgataaagacaccatcgagaagctgaaggagaaaaagctgtcgccgatcacctatccc
121      D  D  K  D  T  I  E  K  L  K  E  K  K  L  S  P  I  T  Y  P
464     cacggactggctctggcaaaggacatagatgctgtaaaatacctggaatgttcagctttg
141      H  G  L  A  L  A  K  D  I  D  A  V  K  Y  L  E  C  S  A  L
524     acccagcggggtctgaagaccgtgttcgacgaggccatcagggccgtcctctgtcctcaa
161      T  Q  R  G  L  K  T  V  F  D  E  A  I  R  A  V  L  C  P  Q
584     cccaccaaggccaagaagaagccctgctccctcctgtaa
181      P  T  K  A  K  K  K  P  C  S  L  L  *
623     attattctcccagacccagaacaagacacgaatttattcatattgatcaaccactgtaac
683     aaatggagcagtgagaaattctgtataaaatttccactagtttagactgcttttgtgttt
743     tcaaaatattcagctcggagcaaaccctgagacgtcagatttagtagagaaaaagaccca
803     ggaccctcacacatacagtattccctttgacccgtgtgtcatttgtttttacgttgttga
863     atcagacacaacactgaaatgtttaaaggcagtttatattcaataatttgagggaatgca
923     gttttgaagctgaatctttttttttttattattccaccaacatttaatttcaaatgtattc
983     ttctctgtgatgttaataaataaaaacatactggtgaaaaaacaaaaaaaaaaaaaaaaa
1043    aaaaa
```

Fig. 1. (*continued*)

structures was 0.13 Å.

The full-length of *CsRac2* cDNA (GenBank accession No. MH085220) was 1047 bp, containing a 43 bp 5′- UTR and a 425 bp 3′-UTR with a poly(A) tail. The ORF of *CsRac2* was 579 bp, encoding a protein of 192 amino acids with a calculated molecular weight of 21.35 kDa and a theoretical pI of 7.91. There is 22 negatively (Asp + Glu) charged residues and 24 positively (Arg + Lys) charged residues. *CsRac2* protein also contains a conserved RHO domain (residues 6–179) (Fig. 1B), which is identical in length to the RHO domain of *CsRac1*. Similar with *CsRac1*, *CsRac2* protein also belongs to a non-transmembrane protein without signal peptide (Figs. S1 B and S2 B). Based on the calculation, *CsRac2* protein contained 64.6% alpha helix, 42.7% beta pleated sheet and 13.0% beta turn (Figs. S3 B). 3D molecular modeling of *CsRac2* was generated based on template of 1ds6.1.A (Fig. S4 B). *CsRac2* showed 94.79% consistency with its template. 181 atoms were involved in the calculation and the root mean square deviation of two superposed structures was 0.06 Å.

3.2. Multiple sequence alignment

Homology analysis revealed that *CsRac1* shared relative high identities (96%) with *Rac1* of *Takifugu rubripes*, *Stegastes partitus*, *Hippocampus comes*, *Maylandia zebra*, *Neolamprologus brichardi*, and so on. *CsRac2* shared relative high identities with *Rac2* of *Paralichthys olivaceus* (99%), *Lates calcarifer* (97%), *Stegastes partitus* (97%) and *Mesocricetus auratus* (96%).

Meanwhile, a multiple sequence alignment revealed that RHO domain was existed in all aligned Rac, which support the conclusion that *Rac1* and *Rac2* are highly conserved in different organisms (Fig. 2).

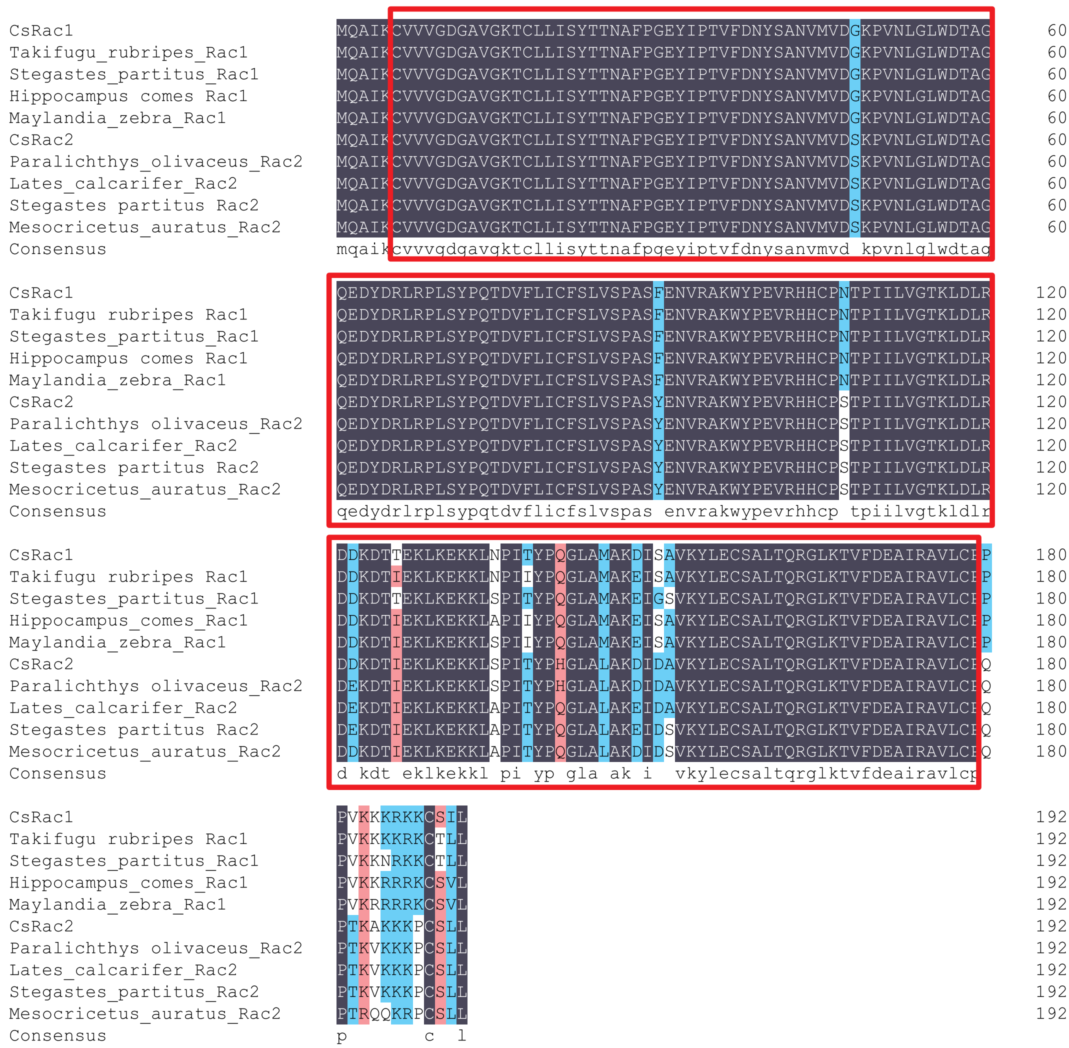

Fig. 2. Multiple sequence alignment of *CsRac1* and *CsRac2* with other counterparts. The RHO domain is shown in the red open boxes. The identical amino acid residues are shaded in black and marked with lowercase letters. (For interpretation of the references to colour in this figure legend, the reader is referred to the Web version of this article.)

3.3. Phylogenetic analysis

A neighbor-joining phylogenetic tree was constructed based on the deduced amino acid sequences of *CsRac1*, *CsRac2* and other counterparts. In general, Rac1 and Rac2 proteins were clustered separately and formed two separated subgroups (Fig. 3). Phylogenetic tree revealed that, *CsRac1* first clustered with Rac1 of *S. partitus* and *Nothobranchius furzeri*, while *CsRac2* first clustered with Rac2 of *P. olivaceus*.

3.4. Tissue distribution of CsRac1 and CsRac2

qRT-PCR was performed to detect different tissue distributions of *CsRac1* and *CsRac2*. *CsRac1* showed the highest expression level in the liver tissue, followed by gill, and less expression in the spleen, brain, kidney, and intestine (Fig. 4A). *CsRac2* transcript was most abundant in gill, with a moderate expression in spleen and kidney, fewer expression in liver, brain and intestine (Fig. 4B).

3.5. Expression pattern of CsRac1 and CsRac2 after bacteria challenge

Based on the results of tissue distribution, we analyzed the temperal expression of *CsRac1* and *CsRac2* in liver and gill in response to pathogenic challenge. Liver and gill were sampled at 0, 12, 24, 48, 72 and 96 h after *V. harveyi* challenge. We found the relative expression of *CsRac1* and *CsRac2* showed certain regularity (Fig. 5). In liver tissue, *CsRac1* was up-regulated to the highest level at 48 h after *V. harveyi* challenge and then gradually declined and leveled off. Meanwhile, the *CsRac2* also firstly up-regulated at 48 h, subsequently down-regulated at 72 h, and finally peaked at 96 h (Fig. 5A). In the gill, the transcript level of *CsRac1* and *CsRac2* showed the same trend. After 12 h post-infection, the mRNA level of *CsRac1* and *CsRac2* presented a slight reduction and then raised to the highest level at 48 h, and then presented a fluctuated decrease at 72 h followed by an increase trend at 96 h.

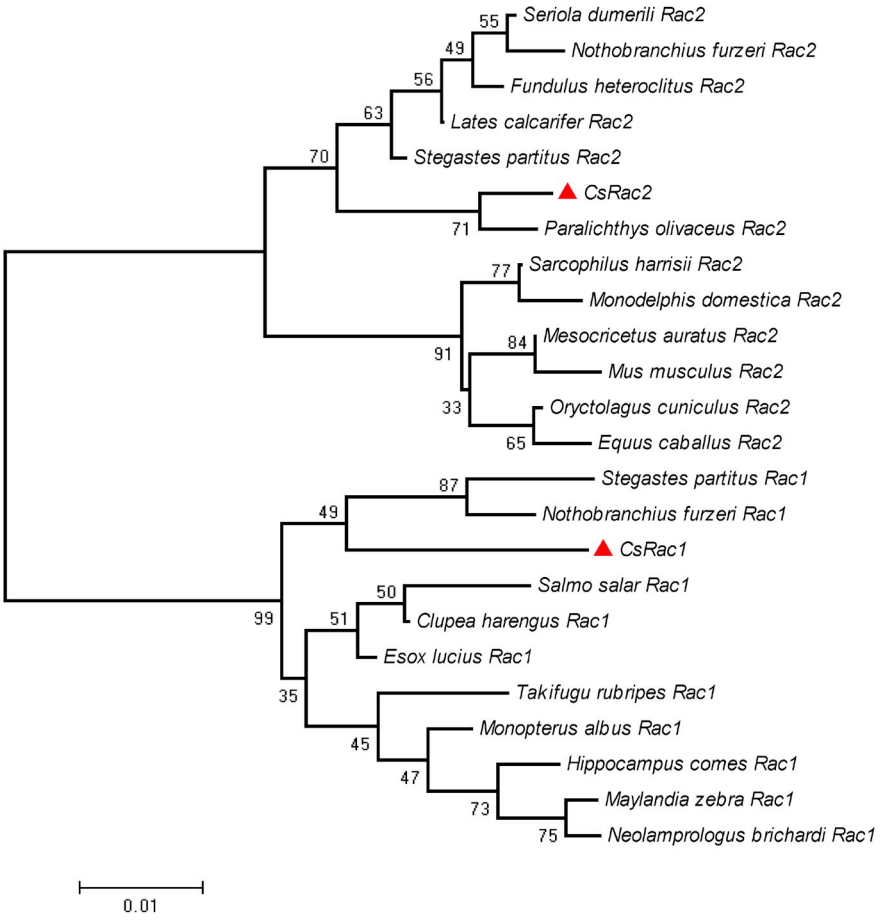

Fig. 3. Phylogenic analysis of *CsRac1* and *CsRac2* with other counterparts. Numbers at branch nodes represent the confidence level of 1000 bootstrap replications. *CsRac1* and *CsRac2* are labeled with a red triangle. The accession number of *T. rubripes* Rac1, *S. partitus* Rac1, *H. comes* Rac1, *M. zebra* Rac1, *N. brichardi Rac1, Esox lucius Rac1, Nothobranchius furzeri Rac1, Salmo salar Rac1, Monopterus albus Rac1, Clupea harengus Rac1, P. olivaceus* Rac2, *L. calcarifer* Rac2, *S. partitus* Rac2, *M. auratus* Rac2, *Seriola dumerili Rac2, Fundulus heteroclitus Rac2, Mus musculus Rac2, Sarcophilus harrisii Rac2, Nothobranchius furzeri Rac2, Oryctolagus cuniculus Rac2, Equus caballus Rac2* and *Monodelphis domestica Rac2* was XP_003961381.1, XP_008301663.1, XP_019726715.1, XP_004562402.1, XP_006801016.1, XP_010904265.1, XP_015801124.1, XP_014049576.1, XP_020471550.1, XP_012694380.1, XP_019958218.1, XP_018540852.1, XP_008279161.1, XP_005067017.1, XP_022620149.1, XP_012705002.1, NP_033034.1, XP_003771174.1, XP_015824205.1, XP_002723584.1 and XP_001500843.1, XP_001366660.1, respectively. (For interpretation of the references to colour in this figure legend, the reader is referred to the Web version of this article.)

3.6. Decreased expression of CsPAK1, CsIL1-β and CsTNF-α in CsRac1 or CsRac2 silenced cell line

qRT-PCR analysis indicated that the expression levels of *CsRac1* and *CsRac2* were significantly reduced after interfered by related siRNA (Fig. 6). The expression of *CsRac1* and *CsRac2* decreased 27.6% and 18.5%, respectively. Following the silence of *CsRac1* and *CsRac2*, the expression of *CsPAK1, CsIL1-β* and *CsTNF-α* were reduced relative to the control group. In *CsRac1*-silenced group, the expression of *CsPAK1, CsIL1-β* and *CsTNF-α* decreased 43.5%, 57.2% and 29.4%, respectively (Fig. 7A). In *CsRac2*-silenced group, the expression of *CsPAK1, CsIL1-β* and *CsTNF-α* decreased 39.9%, 31.1% and 20.1%, respectively (Fig. 7B). These results suggest that *CsRac1* and *CsRac2* may regulate the expression of *CsPAK1, CsIL1-β* and *CsTNF-α*.

4. Discussion

Although *Rac1* and *Rac2* counterparts from humans were often reported, they have only been identified and analyzed in few kinds of fish. Discovering new Rac GTPases from more kinds of fish and studying their immune functions will help to understand the immune process of the aquatic vertebrate. In our study, the *CsRac1* and *CsRac2* were identified and characterized from *C. semilaevis*. In order to understand their potential roles during hosts' immune process, their cDNA sequence, sequence similarity, tissue distribution, mRNA transcriptional profiles after bacterial infection and their effects on expression of other immune genes were detected.

We successfully identified the *CsRac1* and *CsRac2* genes of *C. semilaevis*. Sequence analysis identified that both *CsRac1* and *CsRac2* proteins contain a conserved RHO domain, which is the signature of Rho GTPase subfamily member [21] (Fig. 1) (Fig. 2). The conserved RHO domain of Rac are involved in Rac/$p67^{phox}$ complex formation and NADPH oxidase, and could be divided into N-terminal (residues 22–45) and C-terminal (residues 143–175) [22]. It has been reported that *Rac1* and *Rac2* defend against bacterial infection by activating NADPH oxidase from which reactive oxygen species will generated [23,24]. The binding of Rac with $p67^{phox}$ is a crucial step during the assemble and activation of the NADPH oxidase [25–27]. In the Rac/$p67^{phox}$ complex, interaction between Rac and the *β* hairpin insertion of $p67^{phox}$ accounts for most of the contacts, including interaction of Ala-159Rac/Arg-102p67, Leu-160Rac/Arg-102p67, Asn-26Rac/Arg-102p67, Ser-22Rac/Arg-102p67, Gln-162Rac/Asn-104p67/Asn-26Rac, Thr-25Rac/Asp-108p67; besides, the other direct hydrogen bonds include interaction of Gly-30Rac/Asp-67p67 and Glu-31Rac/Ser-37p67 [22]. As shown in Fig. 3, all of the residues, involved in the interface of Rac/$p67^{phox}$ complex, are conserved between *Rac1* and *Rac2*, based on which it was speculated that there is not any significant discrimination between Rac isoforms by $p67^{phox}$ [22].

In mammals, while *Racl* and *Rac2* proteins shared 92% homology, there are distinct differences in their tissue distributions [28]. *Rac1* is

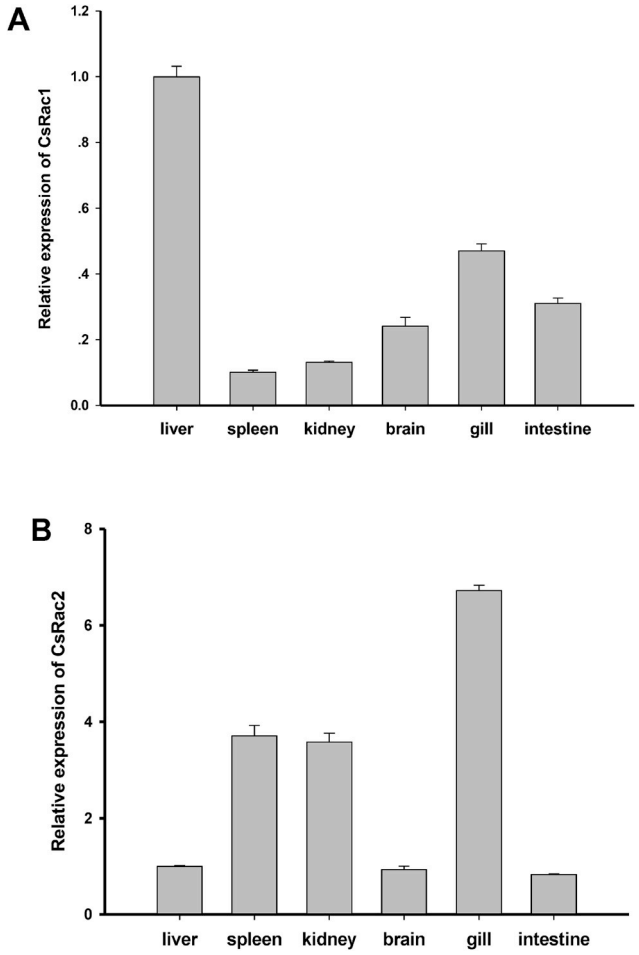

Fig. 4. Tissue distribution of *CsRac1* (A) and *CsRac2* (B) in liver, spleen, kidney, brain, gill and intestine. *Beta-actin* was used as the internal control. Each vertical bar represents the Mean ± S.E. (n = 3).

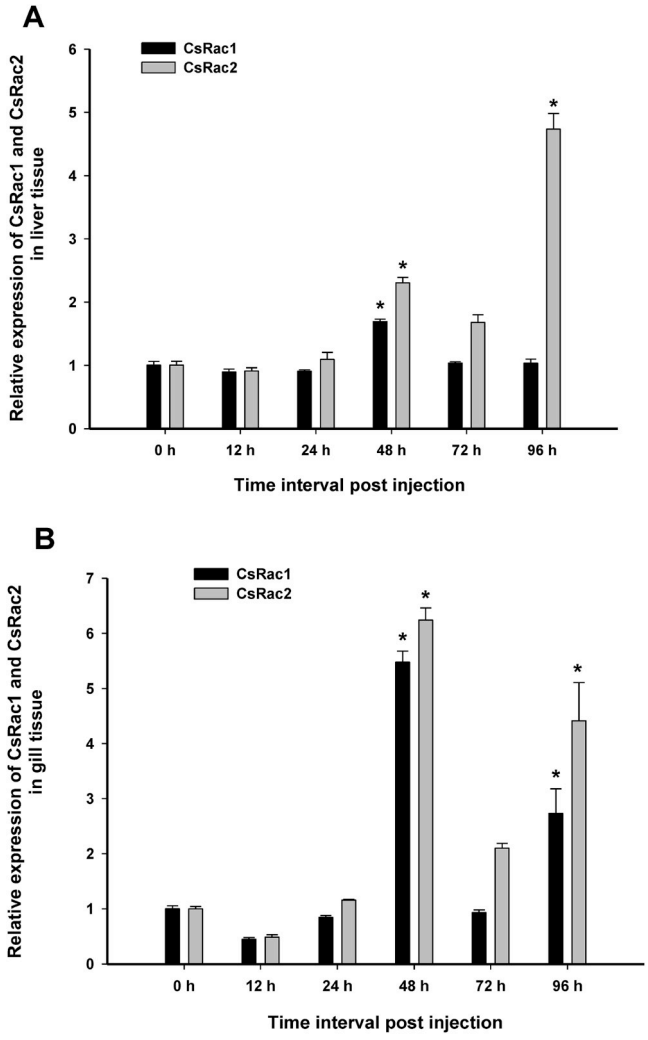

Fig. 5. Expression profile of *CsRac1* and *CsRac2* in the liver(A) and gill(B) at 0, 12, 24, 48, 72 and 96 h after *V. harveyi* challenge. The mRNA levels of *CsRac1* and *CsRac2* were analyzed and standardized according to the *Beta-actin* mRNA levels. Asterisks indicate significant differences ($P < 0.05$) compared with values of the control.

widely distributed, whereas expression of *Rac2* is mainly restricted to hematopoietic tissues [29]. However, in this research, both *CsRac1* and *CsRac2* were expressed in all detected tissues, including liver, spleen, kidney, brain, gill and intestine (Fig. 4). Similar researches have been reported in *Rac1* from *C. idella* [16] and *S. maximus* [17], and *Rac2* from *L. crocea* [20], in which their transcripts showed wide tissue distributions. In teleosts, *Rac1* and *Rac2* exhibited a relative higher expression level in immune-related tissues, for example, *Rac1* of *C. idella* [16], *S. maximus* [17] and *Rac2* of *L. crocea* [20] showed the highest expression level in the liver, gill and head-kidney, respectively. Similarly, the highest expression level of *CsRac1* and *CsRac2* was in liver and gill tissue, respectively. Given the role of *Racl* and *Rac2* in the host's immune response, we speculate that the high expression of *CsRac1* and *CsRac2* in the immune related tissues may be conducive to the protection of half-smooth tongue sole against external invasion. In addition, their different tissue distributions maybe related with their distinct functions in regulation of actin cytoskeleton, chemotaxis, gene transcription, cell growth and so on [30–35].

The time-course analysis showed that *CsRac1* and *CsRac2* were significantly up-regulated in the liver and gill after challenged by *V. harveyi* (Fig. 5). We found that the expression level of *CsRac1* and *CsRac2* peaked at 48 h or 96 h. In other teleost, *Rac1* and *Rac2* also presented fluctuation in immune related tissues, and most of them were dramatically up-regulated [16,17,20]. On the one hand, we speculate that both *CsRac1* and *CsRac2* play important roles during immune responses. The transcription level of *CsRac1* and *CsRac2* was up-regulated significantly at 48 h and 96 h, which maybe related with the two successive processes of phagocytosis and generation of reactive oxygen, respectively. On the other hand, different expression patterns imply that they may perform different functions. It has been illustrated that while both Rac isoforms are required for normal neutrophil chemotaxis, phagocytosis and bacterial killing, they have non-overlapping roles in bacterial phagocytosis and NADPH oxidase function [35]. In fact, Rac2 is much more needed in neutrophil chemotaxis and phagocytosis compared with Rac1, but they could not completely replace the other during neutrophil-mediated bacterial killing [35].

To elucidate the immune roles of *CsRac1* and *CsRac2*, RNA interference was conducted by siRNA method. qRT-PCR results showed that their expression levels were significantly down-regulated. Moreover, all

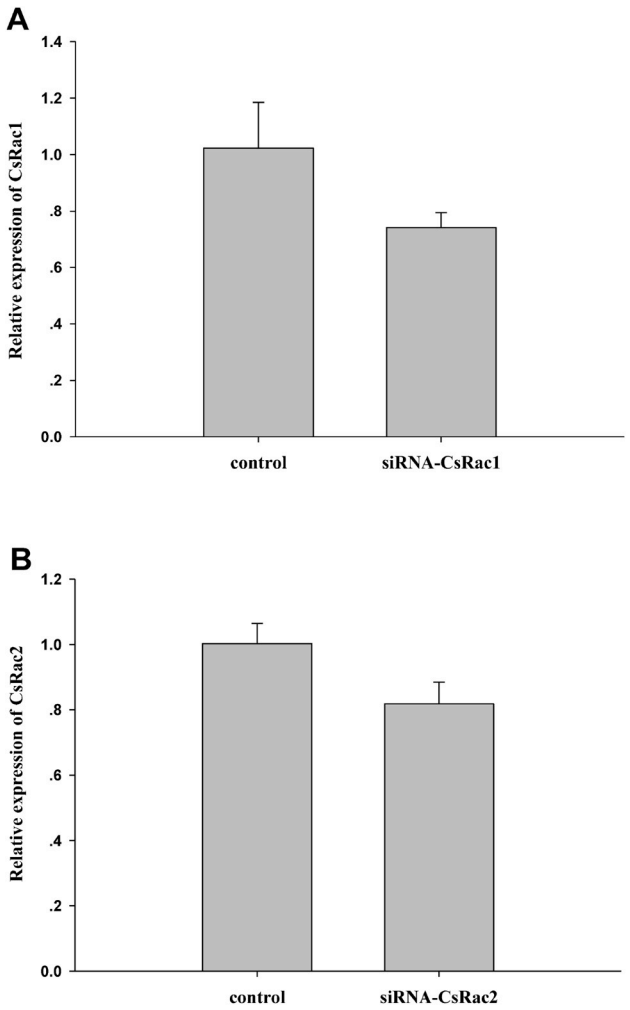

Fig. 6. Expression profiles of *CsRac1* (A) and *CsRac2* (B) after siRNA-mediated RNA interference. Negative control siRNA was transfected as a control. Data are expressed as mean fold changes (means ± S.E., n = 3) relative to the control group.

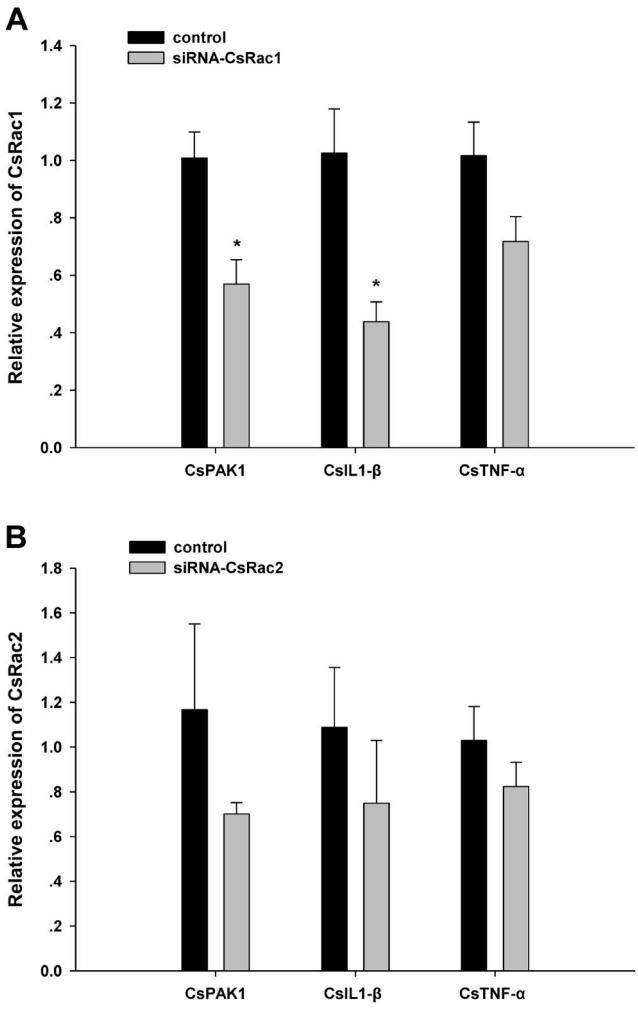

Fig. 7. Relative expression of *CsPAK1, CsIL1-β* and *CsTNF-α* in siRNA-*CsRac1* (A) or siRNA-*CsRac2* (B) transfected cells. Data are expressed as mean fold changes (means ± S.E., n = 3) relative to the control group. Asterisks (*) mark represent significant differences between experimental and control groups.

the expression of *CsPAK1, CsIL1-β* and *CsTNF-α* decreased when *CsRac1* or *CsRac2* was interfered, which suggests that both *CsRac1* and *CsRac2* are positive regulators of *CsPAK1, CsIL1-β* and *CsTNF-α*. Acting as downstream molecules of *Rac1*, *PAK1* play important roles in regulating the *MAP* kinase signaling pathway and a series of cellular processes both in mammals and teleosts [16,36]. It has been elucidated that *PAK1* was strongly suppressed when the *Rac1* of grass carp was suppressed in CIK cells [16] and the expression of *PAK1* was regulated by *Rac1* through *JNK* (Jun NH2-terminal kinase) pathway [37]. In grass carp, over-expression of *Rac1* enhanced expression of cytokines *CsIL1-β* and *CsTNF-α*, in contrast, down-expression of *Rac1* suppressed expression of cytokines *CsIL1-β* and *CsTNF-α* [16]. It was concluded that Rac1 induced the expression of inflammation cytokines such as *IL1-β* and *TNF-α* through NF-kB, thereby protected hosts against pathogenic infection [16]. Combining all these results, we conclude that *CsRac1* and *CsRac2* might play important roles during immune response through increasing the expression of *CsPAK1, CsIL1-β* and *CsTNF-α*.

To sum up, we firstly identified and functionally characterized the cDNA sequences of *CsRac1* and *CsRac2* from *C. semilaevis*. All data observed in this study will provide valuable information to help understanding the functions of Rho GTPase in *C. semilaevis*. Further studies should be carried out to clarify the specific mechanism of Cs*Rac1* and Cs*Rac2* in the innate immune system.

Acknowledgments

This work was supported by the National Nature Science Foundation (31530078), the Central Public-interest Scientific Institution Basal Research Fund, CAFS (NO. 2016HY-ZD0201); the China Agriculture Research System (CARS-47-G03); AoShan Talents Cultivation Program Supported by Qingdao National Laboratory for Marine Science and Technology (No.2017ASTCP-OS15); the Taishan Scholar Climbing Project Fund of Shandong, China, the China Postdoctoral Science Foundation (2015M582171), the Post-Doctoral Applied Research Project Fund of Qingdao City, Applied Basic Research Project of Qingdao City (16-5-1-52-jch), and the fish innovation team of Shandong Agriculture Research System (SDAIT-12-06).

Appendix A. Supplementary data

Supplementary data to this article can be found online at https://doi.org/10.1016/j.fsi.2018.11.006.

References

[1] P. Aspenström, A. Fransson, J. Saras, Rho GTPases have diverse effects on the organization of the actin filament system, Biochem. J. 377 (2004) 327–337.
[2] B. Boettner, A.L. Van, The role of Rho GTPases in disease development, Gene 286 (2002) 155–174.

[3] S. Etienne-Manneville, A. Hall, Rho GTPases in cell biology, Nature 420 (2002) 629–635.
[4] J. Settleman, Rho GTPases in development, Prog. Mol. Subcell. Biol. 22 (1999) 201–229.
[5] A. Hall, Rho GTPases and the actin cytoskeleton, Science 279 (1998) 509–514.
[6] C.D. Nobes, A. Hall, Rho, rac, and cdc42 GTPases regulate the assembly of multimolecular focal complexes associated with actin stress fibers, lamellipodia, and filopodia, Cell 81 (1995) 53–62.
[7] D. Cox, P. Chang, Q. Zhang, P.G. Reddy, G.M. Bokoch, S. Greenberg, Requirements for both Rac1 and Cdc42 in membrane ruffling and phagocytosis in leukocytes, J. Exp. Med. 186 (1997) 1487–1494.
[8] A.W. Roberts, C. Kim, Z. Ling, J.B. Lowe, R. Kapur, B. Petryniak, et al., Deficiency of the hematopoietic cell-specific Rho family GTPase Rac2 is characterized by abnormalities in neutrophil function and host defense, Immunity 10 (1999) 183–196.
[9] A.L. Van, C. D'Souzaschorey, Rho GTPases and signaling networks, Genes Dev. 11 (1997) 2295–2322.
[10] D.J.G. Mackay, A. Hall, Rho GTPases, J. Biol. Chem. 273 (1998) 20685–20688.
[11] F.J. Sangari, J. Goodman, L.E. Bermudez, Mycobacterium avium enters intestinal epithelial cells through the apical membrane, but not by the basolateral surface, activates small GTPase Rho and, once within epithelial cells, expresses an invasive phenotype, Cell Microbiol. 2 (2000) 561–568.
[12] C. Kim, M.C. Dinauer, Rac2 is an essential regulator of neutrophil nicotinamide adenine dinucleotide phosphate oxidase activation in response to specific signaling pathways, J. Immunol. 166 (2001) 1223–1232.
[13] N. Gerasimälk, M. He, D. Cim, N.V. Kuznetsov, E. Severinson, L.S. Westerberg, The small Rho GTPases Rac1 and Rac2 are important for T-cell independent antigen responses and for suppressing switching to IgG2b in mice, Front. Immunol. 8 (2017) 1264.
[14] F. Guo, J.A. Cancelas, D. Hildeman, D.A. Williams, Y. Zheng, Rac GTPase isoforms Rac1 and Rac2 play a redundant and crucial role in T-cell development, Blood 112 (2008) 1767–1775.
[15] A. Avetrochex, J. Perrin, E. Bergeret, M.O. Fauvarque, Rac2 is a major actor of *Drosophila* resistance to *Pseudomonas aeruginosa* acting in phagocytic cells, Gene Cell. 12 (2007) 1193–1204.
[16] M.Y. Hu, Y.B. Shen, X.Y. Xu, H.Y. Yu, M. Zhang, Y.F. Dang, et al., Identification, characterization and immunological analysis of Ras related C3 botulinum toxin substrate 1 (Rac1) from grass carp *Ctenopharyngodon idella*, Dev. Comp. Immunol. 54 (2016) 20–31.
[17] A. Jia, X.H. Zhang, cDNA cloning, characterization, and expression analysis of the Rac1 gene from *Scophthalmus maximus*, Comp. Biochem. Physiol. B Biochem. Mol. Biol. 154 (2009) 80–84.
[18] E. Salas-Vidal, A.H. Meijer, X. Cheng, H.P. Spaink, Genomic annotation and expression analysis of the zebrafish Rho small GTPase family during development and bacterial infection, Genomics 86 (2005) 25–37.
[19] F. Han, X. Wang, Q. Yang, M. Cai, Z.Y. Wang, Characterization of a RacGTPase upregulated in the large yellow croaker *Pseudosciaena crocea* immunity, Fish Shellfish Immunol. 30 (2011) 501–508.
[20] L. Liu, F. Han, Y. Zhang, X. Wang, Z. Wang, J. University, Cloning and analysis of Rac2 gene in disease-resistant in the large yellow croaker(*Larimichthys crocea*), J. Jimei Univ. 22 (2017) 1–11.
[21] A. Hall, Rho family GTPases, Biochem. Soc. Trans. 40 (2012) 1378–1382.
[22] K. Lapouge, S.J. Smith, P.A. Walker, S.J. Gamblin, S.J. Smerdon, K. Rittinger, Structure of the TPR domain of p67phox in complex with Rac.GTP, Mol. Cell 6 (2000) 899–907.
[23] A. Abo, A. Boyhan, I. West, A.J. Thrasher, A.W. Segal, Reconstitution of neutrophil NADPH oxidase activity in the cell-free system by four components: p67-phox, p47-phox, p21rac1, and cytochrome b-245, J. Biol. Chem. 267 (1992) 16767–16770.
[24] F. Niedergang, P. Chavrier, Regulation of phagocytosis by Rho GTPases, Curr. Top. Microbiol. Immunol. 291 (2005) 43–60.
[25] A. Abo, E. Pick, A. Hall, N. Totty, C.G. Teahan, A.W. Segal, Activation of the NADPH oxidase involves the small GTP-binding protein p21rac1, Nature 353 (1991) 668–670.
[26] U.G. Knaus, P.G. Heyworth, T. Evans, J.T. Curnutte, G.M. Bokoch, Regulation of phagocyte oxygen radical production by the GTP-binding protein Rac 2, Science 254 (1991) 1512–1515.
[27] D. Diekmann, A. Abo, C. Johnston, A.W. Segal, A. Hall, Interaction of Rac with p67phox and regulation of phagocytic NADPH oxidase activity, Science 265 (1994) 531–533.
[28] J. Didsbury, R.F. Weber, G.M. Bokoch, T. Evans, R. Snyderman, rac, a novel ras-related family of proteins that are botulinum toxin substrates, J. Biol. Chem. 264 (1989) 16378–16382.
[29] K. Burridge, K. Wennerberg, Rho and Rac take center stage, Cell 116 (2004) 167.
[30] M. Glogauer, C.C. Marchal, F. Zhu, A. Worku, B.E. Clausen, I. Foerster, et al., Rac1 deletion in mouse neutrophils has selective effects on neutrophil functions, J. Immunol. 170 (2003) 5652–5657.
[31] Y. Gu, M.D. Filippi, J.A. Cancelas, J.E. Siefring, E.P. Williams, A.C. Jasti, et al., Hematopoietic cell regulation by Rac1 and Rac2 guanosine triphosphatases, Science 302 (2003) 445–449.
[32] C.X. Sun, G.P. Downey, F. Zhu, A.L. Koh, H. Thang, M. Glogauer, Rac1 is the small GTPase responsible for regulating the neutrophil chemotaxis compass, Blood 104 (2004) 3758–3765.
[33] G. Fenteany, M. Glogauer, Cytoskeletal remodeling in leukocyte function, Curr. Opin. Hematol. 11 (2004) 15–24.
[34] M.C. Dinauer, Regulation of neutrophil function by Rac GTPases, Curr. Opin. Hematol. 10 (2003) 8–15.
[35] A.L.Y. Koh, C.X. Sun, F. Zhu, M. Glogauer, The role of Rac1 and Rac2 in bacterial killing, Cell. Immunol. 235 (2005) 92–97.
[36] S. Zhang, J. Han, M.A. Sells, J. Chernoff, U.G. Knaus, R.J. Ulevitch, et al., Rho family GTPases regulate p38 mitogen-activated protein kinase through the downstream mediator Pak1 (*), J. Biol. Chem. 270 (1995) 23934–23936.
[37] U.G. Knaus, G.M. Bokoch, The p21Rac/Cdc42-activated kinases (PAKs), Int. J. Biochem. Cell Biol. 30 (1998) 857–862.